Consensus-Based Odor Source Localization by Multiagent Systems

Abhinav Sinha, Ritesh Kumar, Rishemjit Kaur, and Amol P. Bhondekar

***Abstract*—This paper presents an investigation of the task of localizing an unknown source of an odor by heterogeneous multiagent systems. A hierarchical cooperative control strategy has been proposed as a potential candidate to solve the problem. The agents are driven into consensus as soon as the information about the location of source is acquired. The controller has been designed in a hierarchical manner of group decision making, agent path planning, and robust control. In group decision making, the particle swarm optimization algorithm has been used along with the information of the movement of odor molecules to predict the odor source location. Next, a trajectory has been mapped using this predicted location of source, and the information is passed to the control layer. A variable structure control has been used in the control layer due to its inherent robustness and disturbance rejection capabilities. Cases of movement of agents toward the source under consensus and parallel formation have been discussed. The efficacy of the proposed scheme has been confirmed by simulations.**

***Index Terms*—Decentralized cooperative control, heterogeneous multiagent systems (MASs), inverse sine hyperbolic reaching law, odor source localization (OSL), robot olfaction, sliding mode control (SMC).**

I. Introduction

RESEARCH in robot olfaction has received wide attention to address many challenges, some of which include detection of hazardous gases in mines, tunnels and industrial setup, search and rescue of victims, forest fire detection and firefighting [1]–[3], etc. Recently, extra-terrestrial odor source localization via autonomous agents has been carried out on Mars [4], [5]. Numerous simple and complex algorithms for olfaction problems have imitated behavior of biological entities, such as mate seeking by moths, foraging by lobsters, prey tracking by mosquitoes and blue crabs, etc. However, techniques like probabilistic inference [6], [7]; robust control [8]; swarm intelligence [9]; biased random walk [10]; and optimization and meta-heuristics prove better in localization than aforementioned techniques.

Works on OSL in early 90s were mostly targeted via chemical gradient-based techniques in a diffusion dominated environment [11]–[14]. Attributed to geometry and dimensions of the above-ground agents, this assumption leads to suboptimal performance. This assumption, however, yields satisfactory performance in underground search [15]–[17]. Difficulties associated with diffusion dominated odor dispersal model led to the development of reactive plume tracking approaches, the performance of which was further improved by combining vision with sensing [18]–[20]. The efficiency of techniques depending heavily on sensing, such as chemotaxis [21]; anemotaxis [6], [22]; infotaxis [7]; fluxotaxis [23] and their close variants are limited by the quality of sensors and the manner in which they are used. Bio-inspired agent maneuvering such as Braitenberg style [24], *E. coli* algorithm [10], zigzag dung beetle approach [25], and silkworm moth style [15], [26], [27] are slow in localization. Many of these localizing techniques deliver unsatisfactory tracking performance in a turbulence dominated environment.

With advantages of multiagent systems such as spatial diversity, distributed sensing and actuation, redundancy, scalability, high reliability, and increased probability of success, OSL can be effectively solved. This dynamical optimization problem is characterized by three stages: 1) instantaneous plume sensing (plume finding); 2) maneuvering of the agents (plume traversal); and 3) cooperative control of the agents. In spite of growing attention from researchers in the last decade [28]–[31], only a few works have addressed OSL using MAS. A distributed cooperative algorithm based on swarm intelligence was put forth by Hayes *et al.* [32] and experimental results proved multiple robots perform more efficiently than a single autonomous robot. Marques *et al.* [33] proposed particle swarm optimization (PSO) algorithm [34] to localize odor source. Studies in [35] reported modified PSO technique based on electrical charge theory by using neutral and charged robots to find the odor source without getting trapped into a local maximum concentration. Cooperative control based on simplified PSO was proposed by Lu *et al.* [36], which is a type of proportional-only controller and the operating region is confined between the global and the local best. This requires complicated obstacle avoidance algorithms and more energy consumption. Odor propagation is nontrivial, i.e., odor arrives in packets, leading to wide fluctuations in measured concentrations. Plumes also tend to be dynamic and turbulent. In order

Manuscript received January 18, 2018; revised May 6, 2018; accepted September 2, 2018. This work was supported by CSIR under Major Lab Project. This paper was recommended by Associate Editor L. Zhang. *(Corresponding author: Abhinav Sinha.)*

A. Sinha is with the Department of Aerospace Engineering, Indian Institute of Technology Bombay, Mumbai 400076, India (e-mail: sinha.abhinav@iitb.ac.in).

R. Kumar, R. Kaur, and A. P. Bhondekar are with V1(b), Post-Harvest Technologies, CSIR–Central Scientific Instruments Organisation, Chandigarh 160030, India (e-mail: riteshkr@csio.res.in; rishemjit.kaur@csio.res.in; amolbhondekar@csio.res.in).

This paper has supplementary downloadable material available at http://ieeexplore.ieee.org, provided by the author.

Color versions of one or more of the figures in this paper are available online at http://ieeexplore.ieee.org.

Digital Object Identifier 10.1109/TCYB.2018.2869224

to effectively solve OSL problem, information of wind needs to be taken into consideration. As odor molecules travel downwind, direction of wind provides an effective information on relative position of the source. Using both concentration and wind information, Lu and Han have designed a particle filter-based cooperative control scheme [37] to coordinate multiple robots toward odor source. However, the dynamical model used in [36] and [37] are oversimplified to integrator dynamics and the effects of unknown perturbations have not been considered. To address the effect of perturbations, robust control protocols have been designed in [8] and [38], but dynamics of the agents is homogeneous, i.e., agents are identical. In practice, it is very difficult to obtain truly homogeneous agents. Even truly homogeneous agents exhibit a tendency to drift toward heterogeneity over time and continued operation.

In spite of rapid developments in sensor technology, availability of faster localization algorithms are still a challenge. Motivated by these studies and in order to effectively address the OSL problem, we have proposed a three-layered hierarchical cooperative control scheme which uses concentration information from swarm, as well as wind information from a measurement model [39] describing movement of filaments to locate the odor source. Information about the source via instantaneous sensing and swarm intelligence is obtained in the first layer. Second layer is designed to maneuver the agents via traditional surging, casting, and searching methods. Third layer is the cooperative control layer and the controller is based on the paradigms of variable structure control [also known as sliding mode control (SMC)], which is known for its inherent robustness and properties to reject disturbances that lie in the range space of input. In the third layer, the information obtained in the first layer is passed as a reference to the tracking controller. A block diagram representation of the proposed scheme has been shown in Fig. 1.

The idea of using a finite time controller is not new, however, we have adopted a different perspective in this paper. To the best of authors' knowledge, SMC technique has been used for the first time in OSL. Novel sliding manifold and reaching law provide faster convergence. The sole idea to use such a control is to guarantee faster convergence, complete disturbance rejection, and steady precision. Moreover, studies in this paper incorporate a large class of systems that may contain unknown inherent nonlinearity and heterogeneity. We summarize our contributions via the following points.

1) Individual autonomous agents may have some inherent nonlinear dynamics. This paper generalizes the problem by taking into account nonlinear dynamics of MAS. When the uncertain function is zero, the dynamics simply reduces to that of an integrator system.
2) Individual autonomous agents might have different dynamics for a practical application. Hence, the consideration of heterogeneous agent dynamics is closer to real situations.
3) The finite time robust controller is based on sliding modes with nonlinear sliding hyperplane and novel inverse sine hyperbolic reaching law. Consequently, the control signal is smooth and reachability to the manifold is fast.

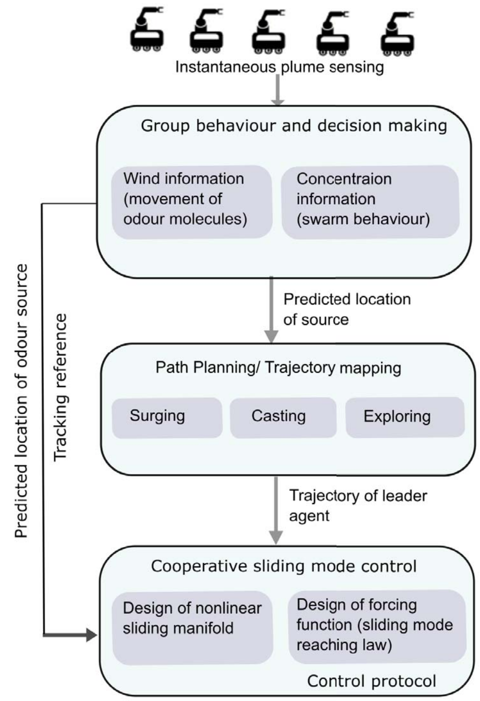

Fig. 1. Proposed hierarchical cooperative control scheme for odor source localization.

4) The synthesized control ensures stability even in the presence of disturbances that are bounded and matched.

After introduction to the study in Section I, remainder of this paper is organized as follows. Section II provides insights into preliminaries of spectral graph theory and SMC. Section III presents dynamics of MAS and mathematical problem formulation, followed by hierarchical decentralized cooperative control scheme in Section IV. Results and discussions have been carried out in Section V, followed by concluding remarks in Section VI. We have provided a supplement to this paper with some additional illustrations to aid the propositions.

II. Preliminaries

A. Spectral Graph Theory for Multiagent Systems

A directed graph, also known as digraph is represented throughout in this paper by $\mathcal{G} = (\mathcal{V}, \mathcal{E}, \mathcal{A})$. $\mathcal{V}$ is the nonempty set in which finite number of vertices or nodes are contained such that $\mathcal{V} = \{1, 2, \dots, N\}$. $\mathcal{E}$ denotes directed edge and is represented as $\mathcal{E} = \{(i, j)\forall i, j \in \mathcal{V}\&i \neq j\}$. $\mathcal{A}$ is the weighted adjacency matrix such that $\mathcal{A} = a(i, j) \in \mathbb{R}^{\mathrm{N}\times\mathrm{N}}$. The possibility of existence of an edge (i, j) occurs if and only if the vertex i receives the information supplied by the vertex j, i.e., $(i, j) \in \mathcal{E}$. Hence, i and j are termed neighbors. The set $\mathcal{N}_i$ contains labels of vertices that are neighbors of the vertex i. For the adjacency matrix $\mathcal{A}$, $a(i, j) \in \mathbb{R}_0^+$. If $(i, j) \in \mathcal{E} \Rightarrow a(i, j) > 0$. If $(i, j) \notin \mathcal{E}$ or $i = j \Rightarrow a(i, j) = 0$. The Laplacian matrix $\mathcal{L}$ [40] is central to the consensus problem and is given by $\mathcal{L} = \mathcal{D} - \mathcal{A}$ where degree matrix, $\mathcal{D}$ is a diagonal matrix, i.e., $\mathcal{D} = \mathrm{diag}(d_1, d_2, \dots, d_n)$ whose entries are $d_i = \sum_{j=1}^{n} a(i, j)$. A directed path from vertex j to vertex i defines a sequence comprising of edges $(i, i_1), (i_1, i_2), \dots, (i_l, j)$ with distinct vertices $i_k \in \mathcal{V}$, $k = 1, 2, 3, \dots, l$. Incidence matrix $\mathcal{B}$ is also a

This article has been accepted for inclusion in a future issue of this journal. Content is final as presented, with the exception of pagination.

diagonal matrix with entries 1 or 0. The entry is 1 if there exists an edge between leader agent and any other agent, otherwise it is 0. Furthermore, it can be inferred that the path between two distinct vertices is not uniquely determined. However, if a distinct node in $\mathcal{V}$ contains directed path to every other distinct node in $\mathcal{V}$, then the directed graph $\mathcal{G}$ is said to have a spanning tree. Consequently, the matrix $\mathcal{L}+\mathcal{B}$ has full rank [40]. Physically, each agent has been modeled by a vertex or node and the line of communication between any two agents has been modeled as a directed edge.

B. Sliding Mode Control

SMC [41] is known for its inherent robustness. The switching nature of the control is used to nullify bounded disturbances and matched uncertainties. Switching happens about a hypergeometric manifold in state space known as sliding manifold, surface, or hyperplane. The control drives the system monotonically toward the sliding surface, i.e., trajectories emanate and move toward the hyperplane (reaching phase). System trajectories, after reaching the hyperplane, get constrained there for all future time (sliding phase), thereby ensuring the system dynamics remains independent of bounded disturbances and matched uncertainties.

In order to push state trajectories onto the surface $s(x)$, a proper discontinuous control effort $u_{\mathrm{SM}}(t,x)$ needs to be synthesized satisfying the inequality

$$s^T(x)\dot{s}(x) \leq -\eta\|s(x)\| \tag{1}$$

with η being positive and is referred as the reachability constant

$$\because\ \dot{s}(x) = \frac{\partial s}{\partial x}\dot{x} = \frac{\partial s}{\partial x}f(t,x,u_{\mathrm{SM}}) \tag{2}$$

$$\therefore\ s^T(x)\frac{\partial s}{\partial x}f(t,x,u_{\mathrm{SM}}) \leq -\eta\|s(x)\|. \tag{3}$$

The motion of state trajectories confined on the manifold is known as *sliding*. Sliding mode exists if the state velocity vectors are directed toward the manifold in its neighborhood. Under such consideration, the manifold is called attractive, i.e., trajectories starting on it remain there for all future time and trajectories starting outside it tend to it in an asymptotic manner. Hence, in sliding motion

$$\dot{s}(x) = \frac{\partial s}{\partial x}f(t,x,u_{\mathrm{SM}}) = 0. \tag{4}$$

$u_{\mathrm{SM}} = u_{\mathrm{eq}}$ is a solution, generally referred as equivalent control, is not the actual control applied to the system but can be thought of as a control that must be applied on an average to maintain sliding motion, and is mainly used for analysis of sliding motion.

III. Dynamics of MAS and Problem Formulation

Consider first-order heterogeneous MAS with a virtual leader and a finite number of followers interacting among themselves and their environment in a well-defined directed topology. Via interagent communication, only local information about the predicted location of source of the odor through instantaneous plume sensing is available. The governing dynamics of first-order heterogeneous MAS that comprise of N agents can be written mathematically as

$$\dot{x}_i(t) = f_i(x_i(t)) + u_{\mathrm{SM}_i}(t) + \varsigma_i;\ i \in [1,N] \in \mathbb{N} \tag{5}$$

where $f_i(\cdot)$ denotes the uncertain dynamics of each agent. x_i and u_{SM_i} are the state of ith agent and the associated control, respectively. ς_i represents bounded exogenous disturbances that enter the system from input channel, i.e., $\|\varsigma_i\| \leq \varsigma_{\max} < \infty$. There is always a limit on how fast a function can change. Considering the functions describing the dynamics (5) do not become infinitely steep at some point, it is safe to assume that the functions satisfy Lipschitz continuity.

Assumption 1: $f_i(\cdot) : \mathbb{R}^+ \times X \to \mathbb{R}^{\mathrm{m}}$ is locally Lipschitz over some domain $\mathbb{D}_{\mathbb{L}}$ with Lipschitz constant $\bar{L}$. For our case, we shall take this domain $\mathbb{D}_{\mathbb{L}}$ to be fairly large. $X \subset \mathbb{R}^{\mathrm{m}}$ is a domain in which origin is contained.

Since the function $f_i(\cdot)$ is uncertain, a nominal system model can be extracted from the known part of the uncertain function $f_i(\cdot)$, and the unknown part can be treated by worst case bounds. The dynamics of each agent is affected by the interconnection among agents as well as the presence of inherent nonlinearity in each agent. Note that when $f_i(\cdot) = 0$, the dynamics reduce to those of integrator systems. Similarly, when $f_i(\cdot)$ are all same, we obtain a set of homogeneous agents.

Remark 1: For the sake of simplicity, we shall carry out the discussion in $\mathbb{R}^1$. However, the same can be extended to higher dimensions by the use of Kronecker products.

Odor molecules tend to disperse heavily in the environment characterized by diffusion. In making assumptions of a diffusion dominated environment, several factors are ignored. A more realistic picture must include effects of wind, turbulence diffusion, and thermal effects. However, effects of turbulence are difficult to be described mathematically. In addition to the effects of wind, the characteristics of environment can also be described by advection phenomenon. Hence, we have considered a diffusion–advection plume model in our discussed source localization problem. Before we begin to use this model, the following assumptions need to be stated.

Assumption 2: We assume near uniform airflow velocity for all time and throughout the domain in which the task of source localization is being performed.

If the domain is characterized by nonuniform airflow velocity, the concentration of odor molecules in a particular region shall vary too rapidly with time and could possibly result in loss of effective sensing, disordering of swarm, and delayed consensus.

Assumption 3: The turbulence diffusion coefficient K needs to be known beforehand via some suitable measurements. In case K is not known beforehand, then K should be estimated or correlated as a function of wind velocity, i.e., $K = f(v_a)$. This estimation can be performed during the experiment with the data obtained through sensors (e.g., anemometers and gas sensors).

Knowledge of these parameters is essential in algorithm research. These parameters influence the overall effective sensing and accuracy of the prediction of odor source location (the global concentration maxima.) The diffusion–advection model provided in [42] and [43] has been recalled here to simulate the dynamic plume under time varying disturbances. A steady concentration profile for a very large span of time ($t \to \infty$) can be written as

$$C(\vec{r}, \infty) = \frac{q_0}{2\pi K d_i} \exp\left\{-\frac{v_a}{2K}(d_i - \vec{r} + \vec{r}_0)\right\}. \tag{6}$$

In (6), $\vec{r}_0 = x_s(t)$ represents the coordinates of the odor source, $d_i = \|x_i - x_s\|$, q_0 is the filament release rate and K is the turbulent diffusion coefficient that is independent of the diffusing material.

The problem of odor source localization can be viewed as a cooperative control problem in which control laws u_{SM_i} need to be designed such that the conditions $\lim_{t\to\infty} \|x_i - x_j\| = 0$ and $\lim_{t\to\infty} \|x_i - x_s\| \le \theta$ are satisfied. Here, x_s represents the probable location of odor source and θ is an accuracy adjustment parameter in declaration of the true location of the source.

IV. Hierarchical Decentralized Cooperative Control Scheme

In order to force the agents in consensus to locate the source of odor, we have come up with the following hierarchical scheme.

A. Group Decision Making

This layer utilizes both concentration and wind information to predict the location of odor source. Thus, the final probable position of the source can be described as

$$\phi(t_h) = k_1 p_i(t_h) + (1 - k_1) q_i(t_h). \tag{7}$$

With the knowledge of PSO, $p_i(t_h)$ in (7) can be described as the oscillation center. Information of the wind is captured in $q_i(t_h)$. $k_1 \in (0, 1)$ denotes additional weighting coefficient.

Remark 2: Since the sensors equipped with the agents can only receive data at discrete instants, the arguments in (7) represent data captured at $t = t_h$ instants ($h = 1, 2, \ldots,$).

It should be noted that ϕ is the tracking reference that is fed to the tracking controller. Now, we present detailed description of obtaining $p_i(t_h)$ and $q_i(t_h)$.

Commonly used simple PSO algorithm can be described in the following form:

$$v_i(t_{h+1}) = \omega v_i(t_h) + u_{\mathrm{PSO}}(t_h) \tag{8}$$
$$x_i(t_{h+1}) = x_i(t_h) + v_i(t_{h+1}). \tag{9}$$

Here, ω is the inertia factor, $v_i(t_h)$ and $x_i(t_h)$ represent the respective velocity and position of ith agent. This commonly used form of PSO can also be used as a proportional-only type controller, however, for the disadvantages highlighted earlier, we do not regard PSO as our final controller. PSO control law, u_{PSO} can be described as

$$u_{\mathrm{PSO}} = \alpha_1(x_l(t_h) - x_i(t_h)) + \alpha_2\big(x_g(t_h) - x_i(t_h)\big). \tag{10}$$

In (10), $x_l(t_h)$ denotes the previous best position and $x_g(t_h)$ denotes the global best position of neighbors of ith agent at time $t = t_h$, and α_1 and α_2 are acceleration coefficients. Since, every agent in MAS can get some information about the magnitude of concentration via local communication, position of the agent with the global best can be easily known. By the idea of PSO, we can compute the oscillation center $p_i(t_h)$ as

$$p_i(t_h) = \frac{\alpha_1 x_l(t_h) + \alpha_2 x_g(t_h)}{\alpha_1 + \alpha_2} \tag{11}$$

where

$$x_l(t_h) = \arg \max_{0<t<t_{h-1}} \{g(x_l(t_{h-1})), g(x_i(t_h))\} \tag{12}$$

$$x_g(t_h) = \arg \max_{0<t<t_{h-1}} \left\{g\big(x_g(t_{h-1})\big), \max_{j\in N} a_{ij} g\big(x_j(t_h)\big)\right\}. \tag{13}$$

Thus, from (10) and (11)

$$u_{\mathrm{PSO}}(t_h) = (\alpha_1 + \alpha_2)\{p_i(t_h) - x_i(t_h)\} \tag{14}$$

which is clearly a proportional-only controller with proportional gain $\alpha_1 + \alpha_2$, as highlighted earlier.

In order to compute $q_i(t_h)$, movement process of a single filament that consists several odor molecules has been modeled based on the study in [39]. If $x_f(t)$ denotes position of the filament at time t, $\bar{v}_a(t)$ represent mean airflow velocity and $n(t)$ be some random process, then the model can be described as

$$\dot{x}_f(t) = \bar{v}_a(t) + n(t). \tag{15}$$

Without loss of generality, we shall regard the start time of our experiment as $t = 0$. From (15), we have

$$x_f(t) = \int_0^t \bar{v}_a(\tau)d\tau + \int_0^t n(\tau)d\tau + x_s(0). \tag{16}$$

$x_s(0)$ denotes the real position of the odor source at $t = 0$.

Assumption 4: We assume the presence of a single, stationary odor source. Thus, $x_s(t) = x_s(0)$.

Presence of a single source implies that there is only one global concentration in the domain. Due to nontrivial nature of odor propagation, discrete packets (or puffs) containing odor molecules are obtained. Since, concentration of each puff can be measured, the global maximum concentration can be established. Implications from Remark 2 require (16) to be implemented at $t = t_h$ instants. Hence,

$$x_f(t_h) = \sum_{m=0}^{t} \bar{v}_a(\tau_m)\Delta t + \sum_{m=0}^{t} n(\tau_m)\Delta t + x_s(t_h) \tag{17}$$
$$x_f(t_h) = x_s(t_h) + \bar{v}_a^\star(t_h) + w^\star(t_h). \tag{18}$$

In (18), $\sum_{m=0}^{t} \bar{v}_a(\tau_m)\Delta t = \bar{v}_a^\star(t_h)$ and $\sum_{m=0}^{t} n(\tau_m) \Delta t = w^\star(t_h)$.

Remark 3: In (18), the accumulated average of $\bar{v}_a^\star(t_h)$ and $w^\star(t_h)$ can also be considered for all possible filament releasing time.

From (18)

$$x_f(t_h) - \bar{v}_a^\star(t_h) = x_s(t_h) + w^\star(t_h). \tag{19}$$

The above relationship, (19) can be viewed as the information about $x_s(t_h)$ with some noise $w^\star(t_h)$. Hence,

$$q_i(t_h) = x_s(t_h) + w^\star(t_h). \tag{20}$$

Therefore, ϕ in (7) can now be constructed from (11) and (20). To summarize, concentration information is obtained via swarm algorithm, and the wind information is obtained using a measurement model that describes the movement of odor

This article has been accepted for inclusion in a future issue of this journal. Content is final as presented, with the exception of pagination.

molecules. Combining this two information together gives the probable location of the odor source, which is fed to the tracking controller.

B. Path Planning

The detection of information of interest based on instantaneous sensing of plume depends on the threshold value of sensors, and the next state is decided according to this threshold. Hence, the blueprints of trajectory planning can be described in terms of the following behavior.

1) *Surging:* If the ith agent receives data well above threshold, we say that some clues about the location of the source have been detected. If the predicted position of the source at $t = t_h$ as seen by ith agent be given as $x_{s_i}(t_h)$, then the next state of the agent is given mathematically as
$$x_i(t_{h+1}) = x_{s_i}(t_h). \tag{21}$$
2) *Casting:* If the ith agent fails to detect information at any particular instant, then the next state is obtained using the following relation:
$$x_i(t_{h+1}) = \frac{\left\| x_i(t_h) - x_{s_i}(t_h) \right\|}{2} + x_{s_i}(t_h). \tag{22}$$
3) *Search and Exploration:* If all the agents fail to detect odor clues for a time segment $[t_h, t_{h+l}] > \delta_0$ for some $l \in \mathbb{N}$ and $\delta_0 \in \mathbb{R}^+$ being the time interval for which no clues are detected or some constraint on wait time placed at the start of the experiment, then the next state is updated as
$$x_i(t_{h+1}) = x_{s_i}(t_h) + F_\sigma^\psi. \tag{23}$$
In (23), F_σ^ψ is some random parameter with σ as its standard deviation and ψ as its mean.

C. Decentralized Control

In the control layer, we design a robust and powerful controller on the paradigms of sliding mode. It is worthy to mention that based on instantaneous sensing and swarm information, at different times, each agent can take up the role of a virtual leader whose opinion needs to be kept by other agents. The trajectory is planned by the leader agent based on surging, casting, and searching behavior. ϕ from (7) has been provided to the controller as the reference to be tracked. The tracking error is formulated as
$$e_i(t) = x_i(t) - \phi(t_h);\ t \in \left[t_h, t_{h+1}\right). \tag{24}$$
In terms of graph theory, we can reformulate the error variable as
$$\epsilon_i(t) = (\mathcal{L} + \mathcal{B})e_i(t) = (\mathcal{L} + \mathcal{B})(x_i(t) - \phi(t_h)). \tag{25}$$
From this point onward, we shall denote $\mathcal{L} + \mathcal{B}$ as $\mathcal{H}$. Next, we propose the nonlinear sliding manifold
$$s_i(t) = \lambda_1 \tanh(\lambda_2 \epsilon_i(t)) \tag{26}$$
which offers faster reachability to the surface. $\lambda_1 \in \mathbb{R}^+$ represents the speed of convergence to the surface, and $\lambda_2 \in \mathbb{R}^+$ denotes the slope of the nonlinear sliding manifold. These are coefficient weighting parameters that affect the system performance. In linear sliding manifolds, the magnitude of error is directly proportional to the magnitude of control effort needed to maintain sliding motion. In order to prevent violations of actuator constraints, the control effort is hard upper and lower bounded by some finite value, thereby making only a portion of the manifold attractive (termed as sliding regime). There is no guarantee of desired performance or stability outside the sliding regime. Moreover, if the reference state is too far from the current system state and the actuator saturates, the controller is unable to cope up, resulting in instability. Hence, it is beneficial to design nonlinear sliding manifolds that can hold the system states regardless of their location in the state space.

In general, traditional sliding mode controllers suffer from an undesirable effect of infinite frequency oscillations, known as chattering [41]. While electronic switching systems may exploit this phenomenon, mechanical hardware may result in wear and tear. Many a times, simulations engines used in numerical analysis and modeling, as well as sampling, switching and delay caused by hardware used to realize the system also introduce chattering and result in excitation of unmodeled high frequency dynamics. This has an adverse effect on system performance like low control accuracy and different losses in circuits and system. Techniques to smoothen the control signal by making continuous approximation of the reaching law via sigmoid functions [44] also exist in literature, but then there is a tradeoff between performance and chattering. Other methods to eliminate chattering include use of higher order sliding mode techniques [45], [46] in which additional hardware is needed to differentiate the control signal. Traditional reaching laws in the literature of sliding mode [41], [47], [48] employ a control effort of fixed gain. In order to shorten the reaching time, a larger control input was designed, leading to chattering. On the contrary, we have designed the gain to be nonlinear by using an inverse sine hyperbolic function. This function is odd and monotonous. Whenever the trajectories are away from the surface, the gain is high and they are pulled toward the hyperplane quickly, and when the trajectories are near the hyperplane, the gain is reduced to avoid chattering. This variable gain in the reaching law results in a smoother control signal as opposed to a discontinuous one. Moreover, interdependence and propinquity of the unwanted chattering phenomenon with controller gain have been obviated [49] (see supplementary material, Section III, p. 3).

The forcing function has been proposed as
$$\dot{s}_i(t) = -\mu \sinh^{-1}(m + w|s_i(t)|)\mathrm{sign}(s_i(t)). \tag{27}$$
In (27), m is a small offset such that the argument of $\sinh^{-1}(\cdot)$ function remains nonzero and w is the gain of the controller. The parameter μ facilitates additional gain tuning. In general, $m << w$. This novel reaching law contains a nonlinear gain and provides faster convergence toward the manifold. Moreover, this reaching law is smooth and chattering free, which is highly desirable in mechatronic systems to ensure safe operation.

Theorem 1: Given the dynamics of MAS (5) connected in a directed topology, error candidates (24), (25) and the sliding manifold (26), the stabilizing control law that ensures accurate reference tracking under consensus can be described as

$$u_{\mathrm{SM}_i}(t) = -\Big\{(\Lambda\mathcal{H})^{-1}\mu\sinh^{-1}(m + w|s_i(t)|)\mathrm{sign}(s_i(t))\Gamma^{-1} + \big(f(x_i(t)) - \dot{\phi}(t_h)\big)\Big\} \tag{28}$$

where $\Lambda = \lambda_1\lambda_2$, $\Gamma = 1 - \tanh^2(\lambda_2\epsilon_i(t))$, $w > \sup_{t\geq 0}\{\|\varsigma_i\|\}$ & $\mu > \sup\{\|\Lambda\mathcal{H}\varsigma_i\Gamma\|\}$.

Remark 4: As mentioned earlier, $\lambda_1, \lambda_2 \in \mathbb{R}^+$. This ensures $\Lambda \neq 0$ and hence its nonsingularity. The argument of $\tanh(\cdot)$ is always finite and satisfies $\lambda_2\epsilon_i(t) \neq \pi\iota(\kappa + 1/2)$ for $\kappa \in \mathbb{Z}$, thus Γ is also invertible. Moreover, the nonsingularity of $\mathcal{H}$ can be established directly if the digraph contains a spanning tree with leader agent as a root.

Proof: From (25) and (26), we can write

$$\dot{s}_i(t) = \lambda_1\Big\{\lambda_2\dot{\epsilon}_i(t)\Big(1 - \tanh^2(\lambda_2\epsilon_i(t))\Big)\Big\} \tag{29}$$

$$= \lambda_1\lambda_2\dot{\epsilon}_i(t) - \lambda_1\lambda_2\dot{\epsilon}_i(t)\tanh^2(\lambda_2\epsilon_i(t)) \tag{30}$$

$$= \lambda_1\lambda_2\dot{\epsilon}_i(t)\Big\{1 - \tanh^2(\lambda_2\epsilon_i(t))\Big\} \tag{31}$$

$$= \Lambda\mathcal{H}\big(\dot{x}_i(t) - \dot{\phi}(t_h)\big)\Gamma \tag{32}$$

with Λ and Γ as defined in Theorem 1. From (5), (32) can be further simplified as

$$\dot{s}_i(t) = \Lambda\mathcal{H}\big(f(x_i(t)) + u_{\mathrm{SM}_i}(t) + \varsigma_i - \dot{\phi}(t_h)\big)\Gamma. \tag{33}$$

Using (27), the control that brings the state trajectories on to the sliding manifold can now be written as

$$u_{\mathrm{SM}_i}(t) = -\Big\{(\Lambda\mathcal{H})^{-1}\mu\sinh^{-1}(m + w|s_i(t)|)\mathrm{sign}(s_i(t))\Gamma^{-1} + \big(f(x_i(t)) - \dot{\phi}(t_h)\big)\Big\}$$

which is same as (28), thereby completing the proof. ■

Remark 5: The control (28) can be practically implemented as it does not contain the uncertainty term.

It is crucial to analyze the necessary and sufficient conditions for the existence of sliding mode when control protocol (28) is used. We regard the system to be in sliding mode if for any time $t_1 \in [0, \infty)$, system trajectories are brought upon the manifold $s_i(t) = 0$ and are constrained there for all time thereafter, i.e., for $t \geq t_1$, sliding motion occurs.

Theorem 2: Consider the system described by (5), error candidates (24), (25), sliding manifold (26), and the control protocol (28). Sliding mode is said to exist in vicinity of sliding manifold, if the manifold is attractive, i.e., trajectories emanating outside it continuously decrease toward it. Stating alternatively, reachability to the surface is ensured for some reachability constant $\eta > 0$. Further, stability can be guaranteed in the sense of Lyapunov if gain μ is designed as $\mu > \sup\{\|\Lambda\mathcal{H}\varsigma_i\Gamma\|\}$.

Proof: Let us take into account, a Lyapunov function candidate

$$V_i = 0.5s_i^2. \tag{34}$$

Taking derivative of (34) along system trajectories yield

$$\dot{V}_i = s_i\dot{s}_i \tag{35}$$

$$= s_i\big\{\Lambda\mathcal{H}\big(f(x_i(t)) + u_{\mathrm{SM}_i}(t) + \varsigma_i - \dot{\phi}(t_h)\big)\Gamma\big\}. \tag{36}$$

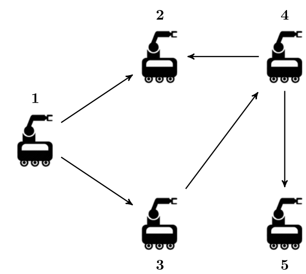

Fig. 2. Topology in which agents are connected.

Substituting the control protocol (28) in (36), we have

$$\begin{aligned}\dot{V}_i &= s_i\Big(-\mu\sinh^{-1}(m + w|s_i|)\mathrm{sign}(s_i) + \Lambda\mathcal{H}\varsigma_i\Gamma\Big)\\ &= -\mu\sinh^{-1}(m + w|s_i|)\|s_i\| + \Lambda\mathcal{H}\varsigma_i\Gamma\|s_i\|\\ &= \Big\{-\mu\sinh^{-1}(m + w|s_i|) + \Lambda\mathcal{H}\varsigma_i\Gamma\Big\}\|s_i\|\\ &= -\eta\|s_i\|\end{aligned} \tag{37}$$

where $\eta = \mu\sinh^{-1}(m + w|s_i|) - \Lambda\mathcal{H}\varsigma_i\Gamma > 0$ is called reachability constant. For $\mu > \sup\{\|\Lambda\mathcal{H}\varsigma_i\Gamma\|\}$, we have

$$\dot{V}_i < 0. \tag{38}$$

Thus, the derivative of Lyapunov function candidate is negative definite confirming stability in the sense of Lyapunov.

Since, $\mu > 0$, $\|s_i\| > 0$ and $\sinh^{-1}(\cdot) > 0$ due to the nature of its arguments. Therefore, (27) and (37) together provide implications that $\forall s_i(0)$, $s_i\dot{s}_i < 0$ and the surface is globally attractive. This completes the proof. ■

V. Results and Discussions

Fig. 2 depicts the interaction topology of the agents [8] as a digraph. In theory, the control has been synthesized using $\mathcal{H}$ matrix. If the elements of $\mathcal{H}$ are constant, the topology is fixed, and if the elements of $\mathcal{H}$ are time-varying, the connection represents a switching topology. Note that although the developed theory and hierarchical scheme can be extended to a switching topology as well, we shall simplify the case by taking a fixed topology.

Assumption 5: Agent 1 appears as the virtual leader to all other agents. Therefore, the topology is fixed and directed.

The associated graph matrices have been described as

$$\mathcal{A} = \begin{bmatrix} 0 & 0 & 1 & 0\\ 0 & 0 & 0 & 0\\ 0 & 1 & 0 & 0\\ 0 & 0 & 1 & 0 \end{bmatrix},\quad \mathcal{B} = \begin{bmatrix} 1 & 0 & 0 & 0\\ 0 & 1 & 0 & 0\\ 0 & 0 & 0 & 0\\ 0 & 0 & 0 & 0 \end{bmatrix},$$

$$\mathcal{D} = \begin{bmatrix} 1 & 0 & 0 & 0\\ 0 & 0 & 0 & 0\\ 0 & 0 & 1 & 0\\ 0 & 0 & 0 & 1 \end{bmatrix},$$

$$\mathcal{L} = \mathcal{D} - \mathcal{A} = \begin{bmatrix} 1 & 0 & -1 & 0\\ 0 & 0 & 0 & 0\\ 0 & -1 & 1 & 0\\ 0 & 0 & -1 & 1 \end{bmatrix},$$

$$\mathcal{L} + \mathcal{B} = \begin{bmatrix} 2 & 0 & -1 & 0\\ 0 & 1 & 0 & 0\\ 0 & -1 & 1 & 0\\ 0 & 0 & -1 & 1 \end{bmatrix}. \tag{39}$$

This article has been accepted for inclusion in a future issue of this journal. Content is final as presented, with the exception of pagination.

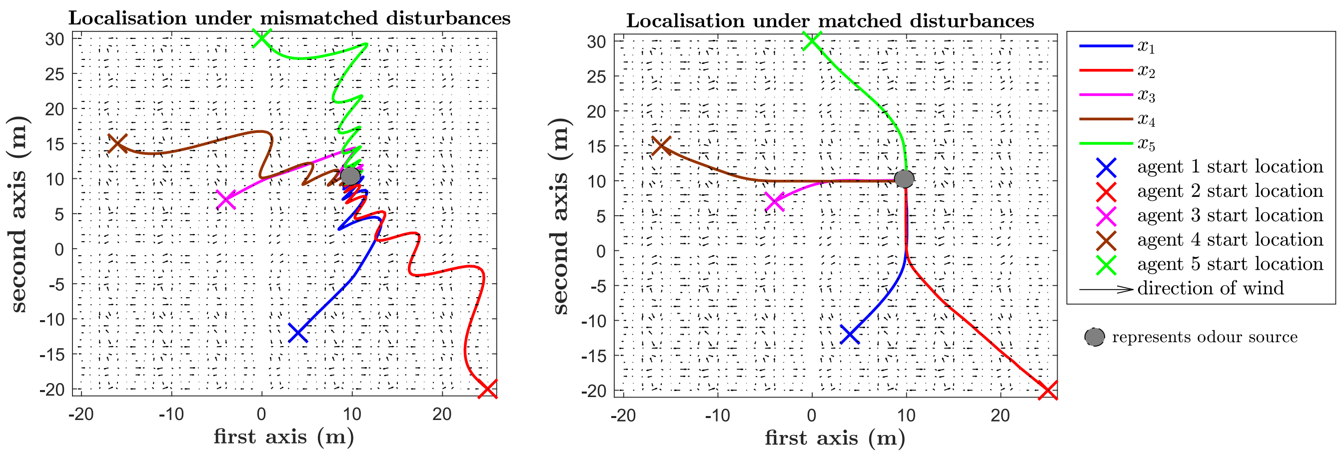

Fig. 3. Localization by MAS under the effect of mismatched and matched disturbances.

TABLE I
VALUES OF THE DESIGN PARAMETERS USED IN SIMULATION

k_1	ω_{max}	α_1	α_2	λ_1	λ_2	μ	m	w
0.5	2 rad/s	0.25	0.25	1.774	2.85	5	10^{-3}	2

TABLE II
FOUR CASES OF LOCALIZATION CONSIDERED IN THIS PAPER

Tech-nique	Con-sensus	Forma-tion	Matched perturbations	Mismatched perturbations
Case 1	✓	×	✓	×
Case 2	×	✓	✓	×
Case 3	✓	×	×	✓
Case 4	×	✓	×	✓

Dynamics of the agents are described as

$$\dot{x}_1 = 0.1\sqrt[3]{\sin(x_1)} + \cos(2\pi t) + u_{\mathrm{SM}_1}(t) + \varsigma_1 \tag{40}$$

$$\dot{x}_2 = 0.1\sin(x_2) - \cos(e^{-x_2 t}) + u_{\mathrm{SM}_2}(t) + \varsigma_2 \tag{41}$$

$$\dot{x}_3 = 0.1\sqrt[3]{\sin(x_3)} + \cos^2(2\pi t) + u_{\mathrm{SM}_3}(t) + \varsigma_3 \tag{42}$$

$$\dot{x}_4 = 0.1\sin(x_4) + \cos(x_4) + u_{\mathrm{SM}_4}(t) + \varsigma_4 \tag{43}$$

$$\dot{x}_5 = 0.1\cos(x_5) - \cos(2\pi t) - e^{-t} + u_{\mathrm{SM}_5}(t) + \varsigma_5. \tag{44}$$

Initial conditions have been chosen to be far from the equilibrium point. We shall consider a time varying disturbance $\varsigma_i = 0.3\sin(\pi^2 t^2)$ for matched case and $\varsigma_i = 20\sin(\pi^2 t^2)$ for mismatched (or, unmatched) case, accuracy parameter $\theta = 0.001$ and maximum mean airflow velocity $\bar{v}_{a_{\max}} = 1$ m/s. Other key design parameters are provided in Table I.

Turbulence coefficient, K, is taken to be 0.02 m^2/s and filament release rate, $q_0 = 2$ mg/s of diffusing substance. We shall present the results for both the cases of localization in $\mathbb{R}^1$ and $\mathbb{R}^2$ to demonstrate the efficiency of the designed control scheme.

For the case of $\mathbb{R}^1$, the odor source is randomly placed between 10 and 11 m (see supplementary material, Section II for illustrations). Agents start from various initial conditions that are far from the origin and progress toward the source via instantaneous plume sensing (by sensing odor molecules, or filaments). As soon as the leader agent senses the odor molecules, the information of predicted next state is exchanged among other agents. This local information is then used to make a consensus while localization. Agents come to consensus in finite time to locate the odor source. In spite of time varying disturbance, the plume tracking is accurate and the localization is successful. Filaments or odor molecules (source information) are released from the odor source and are detected by the sensors equipped with the agents. The tracking controller attempts to minimize the error between the predicted next state and the actual next state. The tracking error lies in the close vicinity of zero as expected, implying that the tracking error has almost been nullified. Norm of tracking errors in $\mathbb{R}^1$ has been depicted in Fig. 4 to depict near nullification of error. Novel sliding manifolds, designed in this paper, also come to consensus in very short span of time, as evident from Fig. 5. It is, then, quite clear that the convergence of state trajectories to the sliding manifold is very fast and is highly desired to ensure a high degree of robustness and autonomy. Such manifolds can also be utilized to attain a desired convergence speed by simple tuning of design parameters. Use of a novel inverse sine hyperbolic reaching law results in a smooth control signals for all the agents. The use of smooth sliding mode controller ensures safe operation in mechatronic devices. Fig. 6 depicts the control signals of all the agents when localization is carried in $\mathbb{R}^1$. It is clear that the signal is chattering free, smooth, and accurate.

Having discussed the case of $\mathbb{R}^1$, we shall now discuss localization in $\mathbb{R}^2$. To avoid confusion between state variable x and axis labeled as x in the usual sense, we have adopted to refer abscissa as first axis and ordinate as second axis throughout this discussion. Agents are driven into consensus to locate the odor source in $\mathbb{R}^2$ in the domain described by the axis limits. Within the domain of localization, a total of 25 trials were done with various initial conditions chosen far from the origin. Fig. 7 shows the average time spent in four cases—localization via consensus under matched perturbations (case 1), localization via formation under matched perturbations (case 2), localization via consensus under mismatched perturbations (case 3), and localization via formation under mismatched perturbations (case 4). Similar to the results in [50], the success rate of this technique is also 100% except

This article has been accepted for inclusion in a future issue of this journal. Content is final as presented, with the exception of pagination.

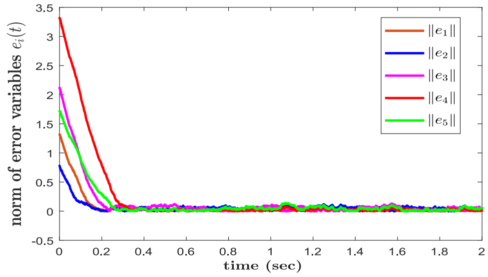

Fig. 4. Localization tracking errors in $\mathbb{R}^1$.

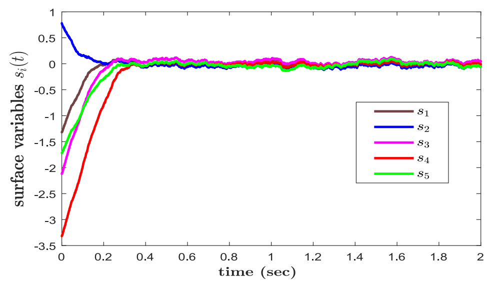

Fig. 5. Sliding manifolds during consensus.

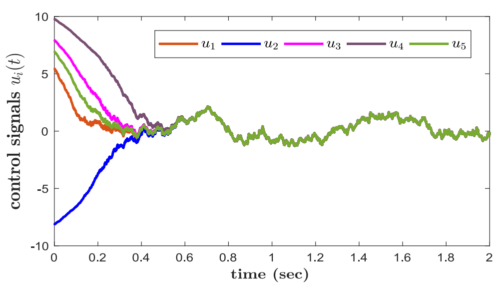

Fig. 6. Smooth control signals of all the agents during consensus.

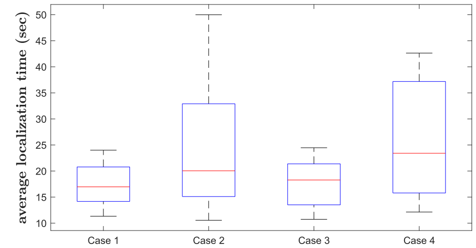

Fig. 7. Average localization time for 25 trials.

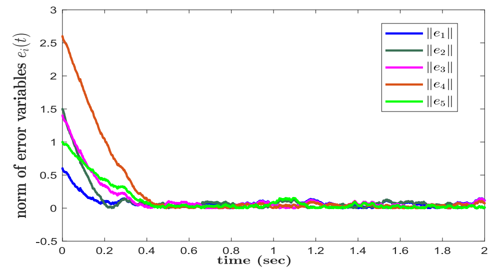

Fig. 8. Localization tracking errors along first axis.

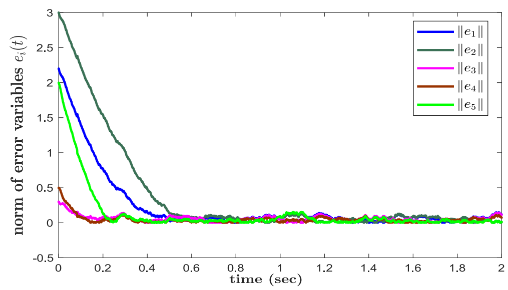

Fig. 9. Localization tracking errors along second axis.

TABLE III
PERFORMANCE METRICS IN CONTEXT OF LOCALIZATION

Technique	Average Success rate	Median localisation Time	Control Implementation
Case 1 (this study)	100%	16 sec	Time-triggered
Case 2 (this study)	100%	20 sec	Time-triggered
Case 3 (this study)	100%	18 sec	Time-triggered
Case 4 (this study)	100%	22 sec	Time-triggered
PSO [33]	21.5%	986.25 sec	Time-triggered
FTMCS [50]	100%	137.5 sec	Time-triggered

for the fact that time spent in localization is lesser via this technique owing to faster convergence of state trajectories to the sliding manifold. The four cases have been illustrated in Table II for ease of reference. A check (cross) mark in a particular column indicates that the particular strategy has been used (not used) in localization.

We shall also present two cases under which localization has been tasked: 1) under consensus and 2) under parallel formation. Note that agents may be subjected to any geometrical pattern, or formation that deems suitable for the task at hand. In Figs. 8 and 9, norms of tracking errors along first and second axis have been depicted. Similar to the error profile in Fig. 4, the tracking is accurate and the agents are able to complete the localization task in finite time. For a random trial, Fig. 3 shows localization in a turbulent environment under the effect of both mismatched and matched disturbances. Under mismatched disturbances and turbulence, localization takes slightly more time as compared with its matched disturbance counterpart. The domain for this task has been set to be a grid of 50×50 along both the axes. Abscissa ranges from -20 to 30, and so does the ordinate. Start position of agents are denoted by a "$\times$" in five different colors. Filaments or the odor molecules are released from the odor source and the molecules disperse in the domain characterized by heavy turbulence. Performance metrics of localization in terms of average time spent in locating the source of odor have been provided in Table III. For best case scenario of localization in $\mathbb{R}^2$, please refer the supplementary material, Section II.

Finally, we state some limitations of the current approach. If the domain of localization is very large, the number of agents should increase in order to effectively solve OSL problem. However, increase in number of agents shall add to the economy, and there is a cost to maintain the communication links. Further, anomalies such as packet dropout, link failure, and latencies in communication should be carefully checked. Another scenario where localization is quite difficult, if not impossible, is the presence of multiple time varying global maxima and local minima. This shall render MAS slightly confused and a different approach should be adopted, such as extrapolating the location based on known (or probable) presence of the source. All these issues shall be addressed in our future studies sequentially.

VI. Conclusion

In this paper, odor source localization via multiagent systems has been addressed. The localizing task is based on a cooperative strategy where agents interact locally among themselves to locate the source of odor in finite time. A hierarchical control scheme has been developed to predict the probable location of odor source using information of wind and concentration. This control scheme based on PSO and SMC is robust and insensitive to matched disturbances. Numerical simulations demonstrate the effectuality of the proposed scheme for both cases 1) when agents localize the odor source via consensus and 2) parallel formation. The localization takes very less time compared to other strategies and the success rate is 100%. In future, we shall address the communication issues associated with the problem.

Competing Interests

The authors declare that there are no competing interests associated with this paper.

References

[1] G. S. Settles, "Sniffers: Fluid-dynamic sampling for olfactory trace detection in nature and homeland security—The 2004 freeman scholar lecture," *J. Fluids Eng.*, vol. 127, no. 2, pp. 189–218, Feb. 2005, doi: 10.1115/1.1891146.

[2] D. W. Gage, "Many-robot MCM search systems," in *Proc. Auton. Veh. Mine Countermeas. Symp.*, 1995, pp. 9–55.

[3] H. Ishida, T. Nakamoto, T. Moriizumi, T. Kikas, and J. Janata, "Plume-tracking robots: A new application of chemical sensors," *Biol. Bull.*, vol. 200, no. 2, pp. 222–226, 2001. [Online]. Available: https://doi.org/10.2307/1543320

[4] V. Formisano, S. Atreya, T. Encrenaz, N. Ignatiev, and M. Giuranna, "Detection of methane in the atmosphere of Mars," *Science*, vol. 306, no. 5702, pp. 1758–1761, 2004. [Online]. Available: http://science.sciencemag.org/content/306/5702/1758

[5] V. A. Krasnopolsky, J. P. Maillard, and T. C. Owen, "Detection of methane in the martian atmosphere: Evidence for life?" *Icarus*, vol. 172, no. 2, pp. 537–547, 2004. [Online]. Available: http://www.sciencedirect.com/science/article/pii/S0019103504002222

[6] J. A. Farrell, S. Pang, and W. Li, "Plume mapping via hidden Markov methods," *IEEE Trans. Syst., Man, Cybern. B, Cybern.*, vol. 33, no. 6, pp. 850–863, Dec. 2003.

[7] M. Vergassola, E. Villermaux, and B. Shraiman, "'Infotaxis' as a strategy for searching without gradients," *Nature*, vol. 445, no. 7126, pp. 406–409, 2007. [Online]. Available: https://hal.archives-ouvertes.fr/hal-00326807

[8] A. Sinha, R. Kaur, R. Kumar, and A. P. Bhondekar, "Cooperative control of multi-agent systems to locate source of an odor," *ArXiv e-prints*, Nov. 2017. [Online]. Available: http://adsabs.harvard.edu/abs/2017arXiv171103819S

[9] X. Cui, C. T. Hardin, R. K. Ragade, and A. S. Elmaghraby, "A swarm approach for emission sources localization," in *Proc. 16th IEEE Int. Conf. Tools Artif. Intell.*, Nov. 2004, pp. 424–430.

[10] C. Lytridis, G. S. Virk, Y. Rebour, and E. E. Kadar, "Odor-based navigational strategies for mobile agents," *Adapt. Behav.*, vol. 9, nos. 3–4, pp. 171–187, Apr. 2001, doi: 10.1177/10597123010093004.

[11] R. Rozas, J. Morales, and D. Vega, "Artificial smell detection for robotic navigation," in *Proc. 5th Int. Conf. Adv. Robot. Unstruct. Environ. (ICAR)*, vol. 2, Jun. 1991, pp. 1730–1733.

[12] V. Genovese, P. Dario, R. Magni, and L. Odetti, "Self organizing behavior and swarm intelligence in a pack of mobile miniature robots in search of pollutants," in *Proc. IEEE/RSJ Int. Conf. Intell. Robots Syst.*, vol. 3, Jul. 1992, pp. 1575–1582.

[13] L. Buscemi, M. Prati, and G. Sandini, "Cellular robotics: Behaviour in polluted environments," in *Proc. 2nd Int. Symp. Distrib. Auton. Robot. Syst.*, 1994.

[14] M. H. E. Larcombe, J. R. Halsall, and Euratom, *Robotics in Nuclear Engineering: Computer-Assisted Teleoperation in Hazardous Environments With Particular Reference to Radiation Fields* (EUR (Series)), Graham and Trotman Ltd., 1984.

[15] R. Russell, "Chemical source location and the RoboMole project," in *Proc. Aust. Robot. Autom. Assoc.*, 2003, pp. 1–6.

[16] R. A. Russell, "Locating underground chemical sources by tracking chemical gradients in 3 dimensions," in *Proc. IEEE/RSJ Int. Conf. Intell. Robots Syst. (IROS)*, vol. 1, Sep. 2004, pp. 325–330.

[17] R. A. Russell, "Robotic location of underground chemical sources," *Robotica*, vol. 22, no. 1, pp. 109–115, 2004.

[18] D. Martinez, L. Perrinet, and D. Walther, "Cooperation between vision and olfaction in a koala robot," in *Proc. Workshop Rep. Neuromorphic Eng.*, 2002, pp. 51–53.

[19] A. Loutfi, S. Coradeschi, L. Karlsson, and M. Broxvall, "Putting olfaction into action: Using an electronic nose on a multi-sensing mobile robot," in *Proc. IEEE/RSJ Int. Conf. Intell. Robots Syst. (IROS)*, vol. 1, Sep. 2004, pp. 337–342.

[20] H. Ishida, K. Yoshikawa, and T. Moriizumi, "Three-dimensional gas-plume tracking using gas sensors and ultrasonic anemometer," in *Proc. IEEE Sensors*, vol. 3, Oct. 2004, pp. 1175–1178.

[21] R. A. Russell, A. Bab-Hadiashar, R. L. Shepherd, and G. G. Wallace, "A comparison of reactive robot chemotaxis algorithms," *Robot. Auton. Syst.*, vol. 45, no. 2, pp. 83–97, 2003. [Online]. Available: http://www.sciencedirect.com/science/article/pii/S0921889003001209

[22] S. Pang and J. A. Farrell, "Chemical plume source localization," *IEEE Trans. Syst., Man, Cybern. B, Cybern.*, vol. 36, no. 5, pp. 1068–1080, Oct. 2006.

[23] D. Zarzhitsky, "Physics-based approach to chemical source localization using mobile robotic swarms," Ph.D. dissertation, Dept. Comput. Sci., Univ. Wyoming, Laramie, WY, USA, 2008.

[24] V. Braitenberg, *Vehicles: Experiments in Synthetic Psychology*. Boston, MA, USA: MIT Press, 1984.

[25] H. Ishida, K. Suetsugu, T. Nakamoto, and T. Moriizumi, "Study of autonomous mobile sensing system for localization of odor source using gas sensors and anemometric sensors," *Sensors Actuators A Phys.*, vol. 45, no. 2, pp. 153–157, 1994. [Online]. Available: http://www.sciencedirect.com/science/article/pii/0924424794008299

[26] L. Marques and A. T. D. Almeida, "Electronic nose-based odour source localization," in *Proc. 6th Int. Workshop Adv. Motion Control*, Apr. 2000, pp. 36–40.

[27] L. Marques, U. Nunes, and A. T. de Almeida, "Olfaction-based mobile robot navigation," *Thin Solid Films*, vol. 418, no. 1, pp. 51–58, 2002. [Online]. Available: http://www.sciencedirect.com/science/article/pii/S004060900200593X

[28] C. W. Reynolds, "Flocks, herds and schools: A distributed behavioral model," *SIGGRAPH Comput. Graph.*, vol. 21, no. 4, pp. 25–34, Aug. 1987. [Online]. Available: http://doi.acm.org/10.1145/37402.37406

[29] W. Ren and R. W. Beard, "Consensus seeking in multiagent systems under dynamically changing interaction topologies," *IEEE Trans. Autom. Control*, vol. 50, no. 5, pp. 655–661, May 2005.

[30] R. Olfati-Saber, J. A. Fax, and R. M. Murray, "Consensus and cooperation in networked multi-agent systems," *Proc. IEEE*, vol. 95, no. 1, pp. 215–233, Jan. 2007.

[31] W. Yu, G. Chen, W. Ren, J. Kurths, and W. X. Zheng, "Distributed higher order consensus protocols in multiagent dynamical systems," *IEEE Trans. Circuits Syst. I, Reg. Papers*, vol. 58, no. 8, pp. 1924–1932, Aug. 2011.

[32] A. T. Hayes, A. Martinoli, and R. M. Goodman, "Swarm robotic odor localization: Off-line optimization and validation with real robots," *Robotica*, vol. 21, no. 4, pp. 427–441, Aug. 2003, doi: 10.1017/S0263574703004946.

[33] L. Marques, U. Nunes, and A. T. de Almeida, "Particle swarm-based olfactory guided search," *Auton. Robots*, vol. 20, no. 3, pp. 277–287, Jun. 2006. [Online]. Available: https://doi.org/10.1007/s10514-006-7567-0

[34] J. Kennedy and R. Eberhart, "Particle swarm optimization," in *Proc. IEEE Int. Conf. Neural Netw.*, vol. 4, Nov. 1995, pp. 1942–1948.

[35] W. Jatmiko, K. Sekiyama, and T. Fukuda, "A PSO-based mobile robot for odor source localization in dynamic advection-diffusion with obstacles environment: Theory, simulation and measurement," *IEEE Comput. Intell. Mag.*, vol. 2, no. 2, pp. 37–51, May 2007.

[36] Q. Lu, S.-R. Liu, and X.-N. Qiu, "A distributed architecture with two layers for odor source localization in multi-robot systems," in *Proc. IEEE Congr. Evol. Comput.*, Jul. 2010, pp. 1–7.

[37] Q. Lu and Q.-L. Han, "Decision-making in a multi-robot system for odor source localization," in *Proc. 37th Annu. Conf. IEEE Ind. Electron. Soc. (IECON)*, Nov. 2011, pp. 74–79.

[38] Q. Lu, S. Liu, X. Xie, and J. Wang, "Decision making and finite-time motion control for a group of robots," *IEEE Trans. Cybern.*, vol. 43, no. 2, pp. 738–750, Apr. 2013.

[39] J. A. Farrell, J. Murlis, X. Long, W. Li, and R. T. Cardé, "Filament-based atmospheric dispersion model to achieve short time-scale structure of odor plumes," *Environ. Fluid Mech.*, vol. 2, no. 1, pp. 143–169, Jun. 2002. [Online]. Available: https://doi.org/10.1023/A:1016283702837

[40] F. R. K. Chung, "Spectral graph theory," in *Proc. CBMS Reg. Conf. Math.*, vol. 92, 1997, p. 212. [Online]. Available: http://bookstore.ams.org/cbms-92

[41] K. D. Young, V. I. Utkin, and U. Ozguner, "A control engineer's guide to sliding mode control," *IEEE Trans. Control Syst. Technol.*, vol. 7, no. 3, pp. 328–342, May 1999.

[42] M. L. Cao, Q. H. Meng, Y. X. Wu, M. Zeng, and W. Li, "Consensus based distributed concentration-weighted summation algorithm for gas-leakage source localization using a wireless sensor network," in *Proc. 32nd Chin. Control Conf.*, Jul. 2013, pp. 7398–7403.

[43] J. Matthes, L. Groll, and H. B. Keller, "Source localization by spatially distributed electronic noses for advection and diffusion," *IEEE Trans. Signal Process.*, vol. 53, no. 5, pp. 1711–1719, May 2005.

[44] A. Sinha and R. K. Mishra, "Nonlinear autonomous altitude control of a miniature helicopter UAV based on sliding mode methodology," *Int. J. Electron. Commun. Technol.*, vol. 6, no. 1, pp. 32–37, Mar. 2015. [Online]. Available: http://www.iject.org/C2E2-2015/7-Abhinav-Sinha.pdf

[45] A. Msaddek, A. Gaaloul, and F. M'sahli, *Output Feedback Robust Exponential Higher Order Sliding Mode Control*. Singapore: Springer, 2017, pp. 53–72.

[46] F. Plestan, V. Brégeault, A. Glumineau, Y. Shtessel, and E. Moulay, *Advances in High Order and Adaptive Sliding Mode Control—Theory and Applications*. Heidelberg, Germany: Springer, 2012, pp. 465–492.

[47] A. Sinha and R. K. Mishra, "Control of a nonlinear continuous stirred tank reactor via event triggered sliding modes," *Chem. Eng. Sci.*, vol. 187, pp. 52–59, Sep. 2018. [Online]. Available: http://www.sciencedirect.com/science/article/pii/S0009250918302719

[48] C. Edwards and S. K. Spurgeon, *Sliding Mode Control: Theory and Applications*. London, U.K.: CRC Press, 1998.

[49] T. Majumder, R. K. Mishra, A. Sinha, S. S. Singh, and P. K. Sahu, "Congestion control in cognitive radio networks with event-triggered sliding mode," *AEU Int. J. Electron. Commun.*, vol. 90, pp. 155–162, Jun. 2018. [Online]. Available: https://www.sciencedirect.com/science/article/pii/S1434841117325438

[50] Q. Lu, Q. L. Han, X. Xie, and S. Liu, "A finite-time motion control strategy for odor source localization," *IEEE Trans. Ind. Electron.*, vol. 61, no. 10, pp. 5419–5430, Oct. 2014.

Abhinav Sinha received the B.Tech. degree in electronics and instrumentation engineering from the Kalinga Institute of Industrial Technology, Bhubaneswar, India, in 2014 and the M.Tech. degree in mechatronics from the Indian Institute of Engineering Science and Technology, Shibpur, India, in 2018.

He is currently a Doctoral Researcher with the Dynamics and Control Group, Department of Aerospace Engineering, Indian Institute of Technology Bombay, Mumbai, India. He was an Assistant System Engineer with the Engineering and Industrial Services Division, Tata Consultancy Services (TCS) Ltd., Mumbai, from 2014 to 2016, where he worked on control system integration, manufacturing execution systems, enterprise manufacturing intelligence, network segmentation, data integration, and data security at plant level. He was also a Visiting Faculty with TCS Global Learning Centre, India, in 2015. From 2017 to 2018, he was a Graduate Researcher with CSIR–Central Scientific Instruments Organisation, Chandigarh, India, where he researched for his master's degree. His current research interests include sliding mode control, event-based control, multiagent systems, cooperative control, and cyber-physical systems.

Mr. Sinha was a recipient of the IEEE Best Paper Award (IEEE Pune Section & IEEE Computer Society) in 2015, On the Spot Award (TCS) in 2015, and the Champions of Initial Learning Programme (TCS) in 2015. He is a member of the International Federation of Automatic Control, Automatic Control and Dynamical Optimization Society, and the Asian Control Association. He currently serves as a Reviewer for *Nonlinear Dynamics* (Springer) and *IET Generation, Transmission and Distribution*.

Ritesh Kumar received the B.E. degree in computer science and engineering from the Manipal Institute of Technology, Manipal, India, in 2009 and the M.Tech. degree in advanced instrumentation and the Ph.D. degree from the Academy of Scientific & Innovative Research, New Delhi, India, in 2011 and 2017, respectively.

Since 2011, he has been a Scientist with CSIR–Central Scientific Instruments Organisation (CSIR–CSIO), Chandigarh, India, working on a number of government and industry-sponsored projects involving various domains of information and communication technology. At CSIR–CSIO, he is also responsible for supervising laboratory and tutorials on machine learning. He has authored and co-authored multiple journal papers. His current research interests include big data analytics, perception modeling, and artificial intelligence.

Mr. Kumar is a member of Digital Olfaction Society and the Institution of Electronics and Telecommunication Engineers.

Rishemjit Kaur received the B.E. degree in electronics (instrumentation and control) from Thapar University, Patiala, India, in 2009 and the M.Tech. degree in advanced instrumentation and the Ph.D. degree from the Academy of Scientific & Innovative Research, New Delhi, India, in 2011 and 2017, respectively.

She was a Research Scholar with Nagoya University, Nagoya, Japan, from 2014 to 2016. Since 2011, she has been a Scientist with CSIR–Central Scientific Instruments Organisation, Chandigarh, India. She received Japanese Government scholarship for research students (MEXT) from 2014 to 2016. Her current research interests include evolutionary optimization techniques, big data analytics, social network analysis, and machine learning.

Dr. Kaur was a recipient of the Genetic and Evolutionary Computation Conference Virtual Creatures Award for her research on developing controller for soft-bodied robots.

Amol P. Bhondekar received the Ph.D. degree in engineering from Panjab University, Chandigarh, India.

He is with CSIR–Central Scientific Instruments Organisation, Chandigarh, where he is a Principal Scientist and the Head of the Department of Agrionics (Post Harvest Technologies). He is also an Associate Professor with the Academy of Scientific and Innovative Research, New Delhi, India. He has number of research articles in reputed journals to his credit. His current research interests include sensors, systems, and development of techniques for artificial organoleptics.

Dr. Bhondekar is a fellow of the Institution of Electronics and Telecommunication Engineers.